GROUND TRUTH LOCATIONS USING SYNERGY BETWEEN REMOTE SENSING AND SEISMIC METHODS - APPLICATION TO EARTHQUAKES IN IRAN AND INDIAN SUBCONTINENT

Chandan K. Saikia[1], Gene A. Ichinose[1], H. -K. Thio[1], Donald V. Helmberger[2], and Mark Simons[2]

URS Group, Inc.[1] and California Institute of Technology[2]

Sponsored by Defense Threat Reduction Agency

Contract No DTRA01-01-C-072

ABSTRACT

This study aims to establish ground truth locations of moderate to large magnitude earthquakes ($4.5 \leq M_w \leq 7$) occurring in Iran, and in and around the Indian subcontinent using both seismic and interferometric synthetic aperture radar methods. To this end, we analyzed seismic waveforms and InSAR (Interferometric Synthetic Aperture Radar) data for one large ($M_w \geq 6$) and two moderate ($5.3 \leq M_w \leq 5.7$) earthquakes in Iran. Similar studies were also conducted for two earthquakes in the Indian subcontinent. One occurred in the northern Himalaya on 29 March 1999 (known as the Chamoli earthquake) and the other occurred in central India on September 29, 1993 (known as the Latur earthquake). For the latter two events, we obtained high quality seismic locations, but interferograms processed using radar data from the European Remote Sensing (ERS) satellites did not produce any discernable surface displacement. Both earthquakes were followed by many aftershocks and were recorded by local temporary stations. For the Chamoli aftershock sequence, we could identify nine aftershocks for which the local network provided good azimuthal coverage and were relocated using an adaptive grid-search location algorithm. Many stations of the Chinese National Network also recorded these aftershocks. We were able to estimate reliable source specific station corrections (SSSCs). The SSSCs from the Chinese stations were, in turn, used in conjunction with other common Incorporated Research Institutes in Seismology (IRIS) and Indian broadband stations to relocate the main event, establishing its location at 30.51±0.045°N latitude and 79.24±0.045°E longitude (depth: 15±1.0 km and origin time: 19h 05m 8.26±1.274s). For the Latur earthquake, local field reports indicated a significant surface deformation, but no deformation could be observed in interferograms because of the large temporal baseline between the radar frames. Using the aftershock data, we were able to conduct a seismic study similar to the Chamoli earthquake to establish its location. For the earthquakes in Iran, the largest event investigated in this study is the Fandoqa earthquake that occurred in Kerman province on 14 March 1998 (M_w 6.6). Our teleseismic P-wave modeling established its depth at 7 km and processing of its InSAR data from the ERS satellites also produced discernable surface displacement. We also identified surface displacements in the processed interferograms for two other earthquakes that occurred in northern and central Iran on 20 June 1997 (lat: 32.254ºN and lon: 60.0278ºE, M_w=5.4) and at the margin of northern and southern Iran on 8 November 1996 (lat: 30.059ºN and lon: 51.006ºE, M_w 5.3). The seismic analysis of the recent BAM earthquake of 26 November 2003 has just been completed. The reliable locations of these events including the others previously established will now allow a reliable calibration of the International Monitoring System (IMS) and other permanent seismic stations available around the study regions.

OBJECTIVES

The goal of this on-going study is to obtain reliable locations for moderate-sized earthquakes (M_w<5.5) in parts of Asia and the Middle East. We will deliver accurate locations, associated waveforms, raw satellite synthetic radar interferometry (InSAR) images, processed InSAR phase maps and ground deformation maps to the Department of Energy Knowledge Base. The study is divided into two parts, seismic and geodetic, which are concerned with identifying ground truth (GT) locations for reference events in regions of monitoring interest. The primary objective is to improve earthquake locations to GT10 or GT5 level of accuracy (i.e., events within 10 or 5 km accuracy in their epicentral locations, respectively) when they apparently satisfy GT25 criteria (Yang and Romney, 1999). The other objective is to utilize geodetic data, including synthetic aperture radar interferometry (InSAR) to establish accurate locations for shallow and moderate-sized seismic events (M_w<5.2) to validate the ground truth (GT) results determined from seismic methods.

The final task of this study combines seismic and geodetic results to validate the GT locations (Foxall et al., 1998; Lohman et al., 2002; Meyers et al., 2002; Saikia et al., 2003; Steck et al., 2002). These locations determined from a combination of InSAR and seismic methods will be used to develop Source-Specific-Station corrections (SSSCs) for the upper-mantle P-wave phase arrivals, which in turn will be used for relocating nearby earthquakes (M_w < 4.5).

RESEARCH ACCOMPLISHED

28 March 1999 Chamoli earthquake, India (M_w 6.5)

In our previous reports, we presented results of analyzing all available seismograms recorded at regional, far-regional and teleseismic distances from this earthquake. Regional seismograms included waveforms recorded by all broadband stations from the Indian subcontinent. Far-regional seismograms included waveforms from the IRIS stations at distances within 10º<_<30º including those from the INDEPTH-III experiment. The teleseismic waveforms were from sixty-six stations and included both the vertical and radial components. Modeling of this entire data set enabled us to establish a robust focal mechanism and depth at 17 km. Theoretical surface deformation was calculated with this new depth and focal mechanism. Our calculation suggested that surface deformation from such an event should be discernable in interferograms processed from the radar data. We acquired European Radar Satellite (ERS) data for this earthquake and analyzed satellite data from both descending and ascending tracks using the Repeat Orbit Interferometry Package, but were unable to identify any discernable co-seismic signals. The epicenter of this earthquake lies in the Lesser Himalayas, a region of high relief and shadowing evident in the digital elevation model (DEM), which could be the reason for this failure.

Although we could not find surface deformation in the radar signal, we revisited P and S travel time data, including the aftershock sequence. By analyzing the local data, we identified four aftershocks; each recorded by more than twelve local stations that lie within 100 km of the epicenter and each having a maximum azimuthal gap not more than 180°. The mainshock was not recorded by any of the local stations at such close proximity. There were about 9 aftershocks, which satisfied this criterion (Figure 1). We relocated these nine events using a new adaptive grid-search algorithm in which the reported P and S waves are treated either as the direct or the Pn (or Sn) phase. Scientists in India also provided locations of these events. Considering these locations as initial locations, we defined a rectangular area (10 x 10 km^2) around them and searched for the best hypocenter. We used the minimization of the root-mean-square (RMS) error in the origin time as the selection criterion for the best location of a given event. The entire 10 x 10 km^2 area was discretized into many cells with a constant cell size (5 x 5 km^2). For each cell, the RMS error in the origin time was estimated for a suite of depths ranging from 3 to 30 km in an interval of 1 km. In Figure 1, we show two locations for each event, one determined in this study and the other determined by Indian scientists. To have a better control on the location, we included stations that are within 300 km of the epicenter.

Of the nine events, we selected four; 9904061937, 9904062046, 9904071549, and 9904071623 that were also included in the Chinese earthquake catalog published by the Bureau of Seismology, Beijing. This catalog included the P and S arrival times from the Chinese National Seismograph Network (CDSN). This study used stations that lie within 20° of the epicenter and this data base was augmented by adding arrival time data reported from regional stations that operate in India, including the station NIL (Nilore) in Pakistan and those in Nepal. All these stations provided a good network of stations that surround each event from all azimuths. For the Chinese stations, we used

the station co-ordinates determined in an earlier study by Dr. Paul G. Richards of Lamont-Doherty Earth Observatory at Columbia University. Using the locations determined in this analysis, we computed average source-specific-station-corrections (SSSCs) for all stations. Note that the first arrivals at stations lying beyond the critical distance were considered to be the classical Pn wave. The SSSCs so estimated at stations at upper-mantle distances, are, therefore, the difference in the travel times between the observed P or S waves (which are really turning rays) and the classical head waves. Thus, when the SSSCs are applied to stations at large distances, we reduce the first arrivals to become the arrival times of the head waves. Using these average corrections and the adaptive grid-search technique, we relocated the four selected events (Table 1) to within 5 km of their true locations. Epicenters are well established, but the depth estimates as indicated by poor resolution are often inferior. Epicenters always converged to the same locations irrespective of the depths.

Table 1. Relocation of four aftershocks for estimating SSSCs

Date	Origin Time hr:mn:ss	Latitude (°N)	Longitude (°E)	Depth (km)
99/04/06	19:37:25.85±0.635	30.375	79.33	21
99/04/06	20:46:42.05±0.647	30.33	79.33	19
99/04/07	15:49:14.90±0.615	30.33	79.375	17
99/04/07	16:23:28.86±0.656	30.375	79.285	19

Error in Latitude and Longitude = 0.045°
Error in depth = 1 km

Note that locations reported by the Bureau of Seismology, Beijing for the events investigated in this study have significant error and are off by 24 to 62 km from our estimated locations.

Next, we have relocated the mainshock and an aftershock (9903281936; m_b=5.2) using the same set of stations and the SSSCs. Table 2 shows the relocations of these events.

Table2. Relocation of the mainshock and its largest aftershock

Date	Origin Time hr:mn:ss	Latitude (°N)	Longitude (°E)	Depth (km)
99/03/28	19:05:08.26±1.274	30.51±0.045	79.24±0.o45	15.0±1.0
99/03/28	19:36:04.17±1.487	30.463±0.045	79.150±0.045	19.0±1.0

We have located the mainshock 15.6 km from the ISC (International Seismological Center) and 14.7 km from the Harvard CMT locations, which are at 30.512°N 79.403°E and 30.38°N 79.21°E, respectively. The ISC and HRV locations are 23 km apart. The aftershock is also mislocated by these organizations by about 27 km.

We emphasized locating the mainshock because it is a large event in the Himalayan foothills, and its accurate location can provide means to calibrate 3D models (Ritzwoller et al., 2002) for the structure of the Tibet and Indian subcontinent for future monitoring of the Comprehensive Test Ban Treaty. This new location can improve the locations of other events in the neighborhood of the Chamoli earthquake.

29 September 1993 Latur earthquake, India

This is a large earthquake that occurred 200 km northwest of Hyderbad in Peninsular, India, on 29 September 1993 (22h:25m:48.5s, 18.066ºN 76.451ºE, Mw=6.1, ISC). According to Seeber et al. (1996), this is a very shallow earthquake (h=2.6 km), occurred on a southeast dipping (46º) fault and produced significant surface deformation. Kagami et al. (1994) also indicated that this event is shallow. Based on the analysis of teleseismic waveforms, the existence of localized fractures on the surface and the depth distribution of aftershocks, they suggested that most of the seismic energy was released at very shallow depth and the rupture propagated over a very small source area in a very short time, involving a high stress drop during the rupture process. We also analyzed the teleseismic data. By integrating the high stress condition at the source, we also found, based on modeling of teleseismic P waves at 21 stations, this event to have a depth about 6 km (Figure 2a). An event of this size occurring at such shallow depth is

an ideal candidate for satellite data analysis. Additionally, its epicentral area is in the Deccan Plateau, which is nearly flat. The top and bottom left panels in Figure 3 show the line-of-sight (LOS) and total displacement field calculated for one of the nodal planes obtained by teleseismic P-wave modeling (Figure 2b). The top and bottom right panels show the LOS and total displacement field based on the second nodal plane. Based on those calculations, we expected to observed surface deformation of about ±5 cm, but surface deformation could not be identified in the processed interferogram for this event even though the DEM, which was processed from the Shuttle Radar Topography Mission (SRTM) "*.hgt" files was of adequate quality. The radar data used scenes from tracks and frames that encompass the area where the surface deformation was observed by the reconnaissance team following the earthquake (Seeber et al., 1996). One reason for failing to observe the surface deformation is probably the temporal baseline, which is 3 years. The surface deformation may have been masked by flooding of the Tirana River in the epicentral region and new vegetation. We had one pair of satellite data with a temporal baseline of 8 months, but the data were noisy. Although the satellite data could not help us, we continued further investigation using seismic data from a German task force that installed temporary stations that operated in the epicentral region from 10 October 1993 to 20 January 1994. This network included 11 analog, 5 digital and 4 strong-motion instruments. This network recorded many aftershocks of which three aftershocks were reported in the ISC bulletin (Table 3).

Table 3. Locations for three aftershocks of the Latur earthquake (ISC)

Date	Origin Time hr:mn:ss	Latitude (°N)	Longitude (°E)	Depth (km)	nsta/Az Gap
93/11/12	13:27:28.99±2.91	18.0884	76.5309	14.5	48/94º
93/11/18	14:01:32.07±1.04	18.3600	76.8755	33.0f	9/114
93/11/24	14:45:57.74±0.78	18.1818	76.3833	10.0f	8/116º
Locations based on the Local Network Data					
93/11/12	13:27:31.75	18.00083	76.5442	2.5	15/81º
93/11/18	14:01:27.38	18.00083	76.027	8.5	9/110º
93/11/24	14:46:01.71	18.03367	76.5310	5	12/95º

f=fixed, nsta=Number of Stations, Az Gap=Azimuthal Gap

Of the three aftershocks, the largest one occurred on 12 November 1993 (m_b 4.5), and was recorded by a large number of stations extending up to teleseismic distances (R<69º). We used the network location to estimate SSSCs and relocate the main earthquake.

Earthquakes in Iran

In our previous reports (Saikia et al., 2002, 2003), we presented both seismic and InSAR analyses results for several earthquakes in southern Iran. These earthquakes were of small magnitude (M_w < 5). Only one regional and a few stations at upper-mantle distances recorded these earthquakes. In this study, we have further analyzed satellite data for additional earthquakes that occurred in different parts of Iran. Of all the events for which satellite data were analyzed, we were successful in identifying surface deformation for three events. In the following, we present results of one earthquake from our previous studies and then present results for these new earthquakes.

Figure 3 shows interferograms for the 30 April 1999 earthquake (M_w 4.8) formed using radar images for track 20/frame 3051 (99/04/21-99/05-26) and for track 249,/frame 3051 (99/04/02-99/06/11). The surface deformation generated by this earthquake is observed in the upper right of the image at location of 27.87°N and 53.610°E as two circular interferometric fringes. Based on the waveform analysis, we were able to constrain its depth to 4-6 km. While the centroid depth could not be resolved to within ±10 km using the long-period data, the depth resolution improved significantly by using the broadband P waves from stations in the upper-mantle. The latter analysis yielded depth consistent with the results obtained by modeling the surface deformation observed in satellite data. We should note that the ISC and other organizations estimated its depth deeper than 30 km. The seismic depth and InSAR location were used to estimate origin time and Source Specific Station Corrections (SSSCs) for regional and teleseismic stations. These SSSCs were, in turn, used to relocate 11 other events in the proximity of this earthquake.

In order to extend this study to larger earthquakes, we analyzed both seismic and satellite data for the 13 April 1998

Fandoqa earthquake (M_w 6.6). This is a large earthquake, which produced 23 km of surface faulting with up to 3 m right-lateral strike-slip and 1 m of vertical offsets (Berberian et al., 2001). Berberian et al. also analyzed the satellite data relevant to this earthquake, primarily to understand the triggering of slip on the thrust system and the active tectonics in the associated fault zone. We are currently analyzing its seismic and satellite data together for establishing the ground truth location along with the uncertainty associated with the inferred location. We have modeled the teleseismic P waves (Figure 4, left panel) to constraint the depth at 7-km.

We have successfully processed satellite data acquired from orbits 5714 and 17738 and from track 349/frame 2961 on 24 May 1996 and 11 September 1998, respectively and identified several elliptical fringes at the geographical coordinates 32.1579°N and 59.814°E. Using this location as the focus and by searching through the ISC catalog over an 80 km x 80 km area, we found 9 earthquakes to occur during the span of the satellite data. Of these, two earthquakes that occurred on 20 June 1997 (12h57m36.22s, 32.3269°N 60.0240°E, 34.8 km, ISC, HRV M_w 5.6, M_o=4.2x10^{25} dyne-cm) and 4 April 1998 (15h00m53.00s, 32.4338°N 60.0857°E, h=33.0 km (fixed), ISC, HRV M_w=5.8, M_o=2.42x10^{25} dyne-cm) had M_w larger than 5.5. Based on the teleseismic modeling of P waves, the June event has a depth of 9 km (Figure 4, right panel). The Harvard (HRV) depth for this event is 15 km. We are now analyzing the teleseismic waveform for the April event. A comparison of the waveforms at common stations suggests that both these events are shallow. The April event, which is larger by a factor 2, is shallower based on the damage reports alone. While only 60 houses were damaged in Khorasan Province during the June event, at least 12 people were killed, 10 injured and 600 houses severely damaged in the Birjand-Gonabad area (located east of the Khorasan) during the April event. We have further collected waveforms from stations operating in upper-mantle distances with good signal-to-noise ratios. Modeling of these data has yet to be completed, following which we will be able to associate the surface deformation in satellite data with one or both of these events. Since both events are of moderate size and recorded by more than 100 stations, they will provide useful parameters for the calibration of the region.

Another event analyzed for ground truth is the 25 June 1997 (19h:38m:406s, 33.9380°N 59.4750°E, h=10km, NEIC; HRV M_w=5.9, M_o=7.4x10^{25} dyne-cm) earthquake, which occurred 100 km north of the 20 June 1997 and 10 April 1998 earthquakes. Our teleseismic modeled depth is similar to the depths reported in the NEIC and Harvard catalogs. Because of its shallow depth, we expected the surface deformation caused by this earthquake to be discernable on interferograms from the satellite data. As expected, interferograms showed some surface deformation, but the fringes appeared to have added contributions from the large M_w 7.2 Zirkuh (Qa'enant) earthquake of 10 May 1997, thus requiring further analysis toward establishing the location. In addition to these earthquakes, we processed satellite data acquired on 23 May 1996 and 10 September 1998 (frame 2997). The interferogram showed fringes at a location extending from 30.0901°N latitude/50.9873°E longitude to 30.0376°N latitude/51.0390°E longitude. Searching the NEIC earthquake catalog within a 50 x 50 km^2 area around this location, we identified 11 earthquakes with m_b ranging from 3.9 to 5.0, of which four events occurred in a single day on 11 January 1998 about 40 km away. Their m_b varies between 4.7 and 5.0 and depths between 5 km and 70 km. In our earlier study (Saikia et al., 2003), we noted that locations of such small events may be off by several tens of kilometers and the depths are often shallow compared to those presented in the catalog because of the limited access to local network data.

Our final analysis is the recent BAM earthquake of 26 December 2003 (01h:56m:58.10s) in Iran. This event has been subject to several studies (Fielding et al., 2004, Talebian et al., 2004). We have also pursued a study of its rupture process using seismic data to establish a seismic slip model (Figure 5). We intend to invert the seismic data along with the InSAR deformation to constrain the hypocenter using the method discussed in Saikia et al. (2004). We have also used the local SSSCs that were previously established by Saikia et al. (2003) to find its seismic location, this moved the location toward the location determined by the International Data Center (IDC) and away from the Harvard and our own location determined without using SSSCs

CONCLUSIONS AND RECOMMENDATIONS

Estimating accurate ground truth locations for earthquakes is difficult in areas where seismic network stations are sparse or inaccessible. The addition of InSAR data can overcome this difficulty and provide accurate ground truth locations. Earthquakes that do not produce surface rupture may still generate measurable surface deformation observed from processed radar images acquired before and after the event. However, atmospheric noise or topographical uncertainty may have a correlation length smaller than the regular coherence estimation window,

which may prevent retrieval of useful InSAR signals from processed interferograms. Nevertheless, when ground deformation is discernable in satellite data, hypocenter locations of seismic events can be reliably estimated within the error of the fault dimensions (for M 5 earthquake this is about 2-5 km).

Processing of satellite data for earthquakes occurring in the Indian subcontinent did not produce interferograms where surface deformation could be identified. Often the temporal baseline for the available radar data spans over several years during which natural phenomena seem to mask the surface deformation that may have been caused by the earthquakes. We were able to identify surface deformation on interferograms for several earthquakes in different parts of Iran with magnitude ranging from 4.8 to 7.5.

We found the previously established SSSCs based on ground truth locations using synergy between the seismic and InSAR method useful in the relocation of large earthquakes. Although moderate to large shallow earthquakes (M_w > 5.5-6) have large fault dimensions, they are the earthquakes that often produce discernable surface deformation in interferograms formed from the satellite data. Future study should focus on such earthquakes for providing reliable locations for calibration.

REFERENCES

Berberian, M., Jackson, J. A., Fielding, E., B. E. Parsons, Priestley, K., Qorashi, M., Talebia, M., Walker, R., T. J. Wright, and Baker, C. (2001). The 1998 March 14 Fandoqa earthquake (Mw 6.6) in Kerman province, southeast Iran: re-rupture of the 1981 Sirch earthquake fault, triggering of slip on adjacent thrusts and the active tectonic of the Gowk fault zone, Geophys. J.. Int., 146, 371-398.

Fielding, E. J., T. J. Wright, J. Muller, B. E. Parsons, R. Walker (2004). A seismic deformation of a fold-and-thrust belt imaged by synthetic aperture radar interferometry near Shahbad, southeast Iran, Geol. Soc. Am., V32, N7, 577-580.

Foxall, B., J. J. Sweeny, and W. R. Walter (1998). Identification of mine collapses, explosions and earthquakes using InSAR: a preliminary investigation, in Proceedings of the 20th Annual Seismic Research Symposium., Monitoring Comprehensive Test Ban Treaty (CTBT), 21-23 September, pp. 408-416.

Kagami, H., Kuge, K., Bhartia, B. K., and Sakai, S. (1994). Reconnaissance Report: On the 30 September 1993 Earthquake in the State of Maharastra, India, Research report on Natural Disaster, Japanese Ministry of Education, Science and Culture, No. B-5-4, 88p

Lohman, R. B., M. Simons and B. Savage (2002). Location and mechanism of the Little Skull Mountain earthquake as constrained by satellite radar interferometry and seismic waveform modeling, J. Geophys. Res., 107,10.1029/2001JB000627. ETG, 7-1 to 7-8.

Myers, S., M. Flanagan, M. Pasyanos, W. Walter, P. Vincent and C. Shultz (2002). "Location Calibration in Western Eurasia and North Africa: Ground Truth Improved Earth Models, Bayesian Kriging, Regional Analysis, Location Algorithms, Array Calibration and Validation", in *Proceedings of the 24th Seismic Research Review - Nuclear Explosion Monitoring: Innovation and Integration*, LA-UR-02-5048, Vol. I, pp. 351-360.

Saikia, C. K., R. Lohman, G. Ichinose, D. Helmberger, M. Simons and P. Rosen (2002). Ground truth locations - A synergy of Seismic and Synthetic Aperture Radar Interferometric Methods, 24th Seism. Res. Rev., Nuclear Explosion Monitoring: Innovation and Integration, Sept 17-19, p420-429.

Saikia, C. K., R. Lohman, G, Ichinose, and M. Simons (2003). "Ground Truth Location using a Synergy Between InSAR and Seismic Methods", in *Proceedings of the 25th Seismic Research Review, Nuclear Explosion Monitoring: Building the Knowledge Base*, LA-UR-03-6029, Vol. I, pp. 324-333.

Saikia, C. K., Chen, J., G. A. Ichininose, D. V. Helmberger and M. Simons (2004). "Ground Truth Locations using Synergy Between Remote Sensing and Seismic Method – Application to Chinese Earthquake", *26th Seismic Research Review: Trends in Nuclear Explosion Monitoring*, Orlando, FL (Sept. 21-23, 2004).

Seeber, L, Ekstrom, G., Jain S. K., Murty, C. V. R., Chandak, N., and Armsbruster, J. G. (1996). The 1993 Killary earthquake in central India: A new fault in mesozoic basalt flows, J. Geophys. Res., 101, B4, 8543-8560.

Steck, L. H. Hartse, C. Bradley, C. Aprea, A. Velesco, G. Randall, and J. Franks (2002). "Regional Location Calibration in Asia", in *Proceedings of the 24th Seismic Research Review - Nuclear Explosion Monitoring: Innovation and Integration*, LA-UR-02-5048, Vol. I, pp. 430-439.

Talebian, M., E. J. Fielding, G. J. Funning, M. Ghorashi, J. Jackson, H. Nazari, B. Parsons, K. Priestley, P. A. Rosen, R. Walker, and T. J. Wright (2004). The 2003 Bam (Iran) earthquake: Rupture of a blind nstrike-slip fault, Geophys. Res. Lett., 31, L11611-.

Yang, X. and C. Romney (1999). PIDC ground truth event (GT) database (revision 1), CMR Tech Rept, CMR-00/15.

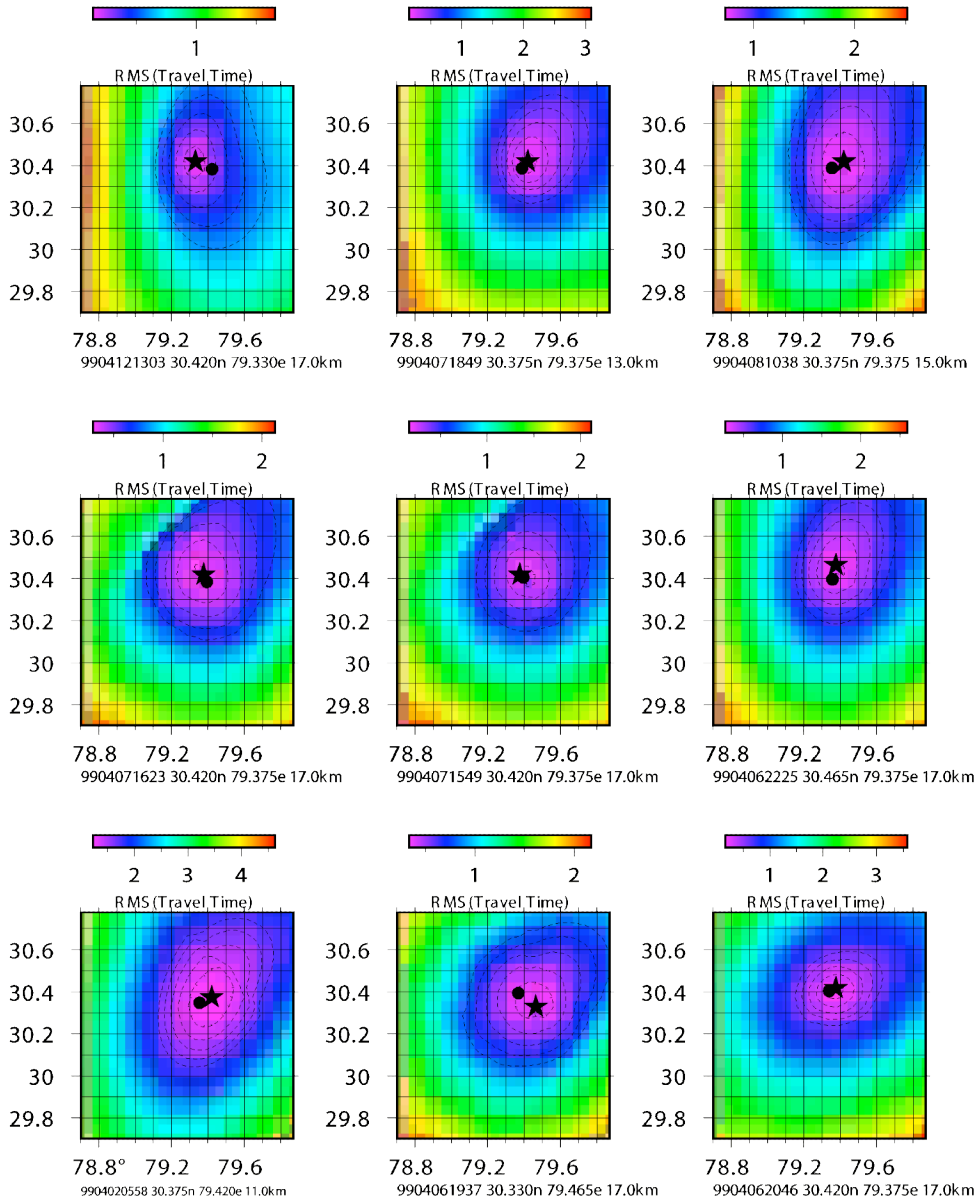

Figure 1 Relocations of nine aftershocks of the March 29, 1999 Chamoli earthquake using our adative grid search algorithm. Events identified as YYMMDDHRMM where YY stands for the year, DD for the month and MM for the day. Stars are the new locations and solid circles are the corresponding locations provided by the scientists in India. The initial contour surrounding the epicenter gives the area over which the RMS (root-mean- squares) origin time error remains same and is minimum, thus essentially corresponds to the uncertainty in the location. The other contours are plotted in an interval of 0.1s.

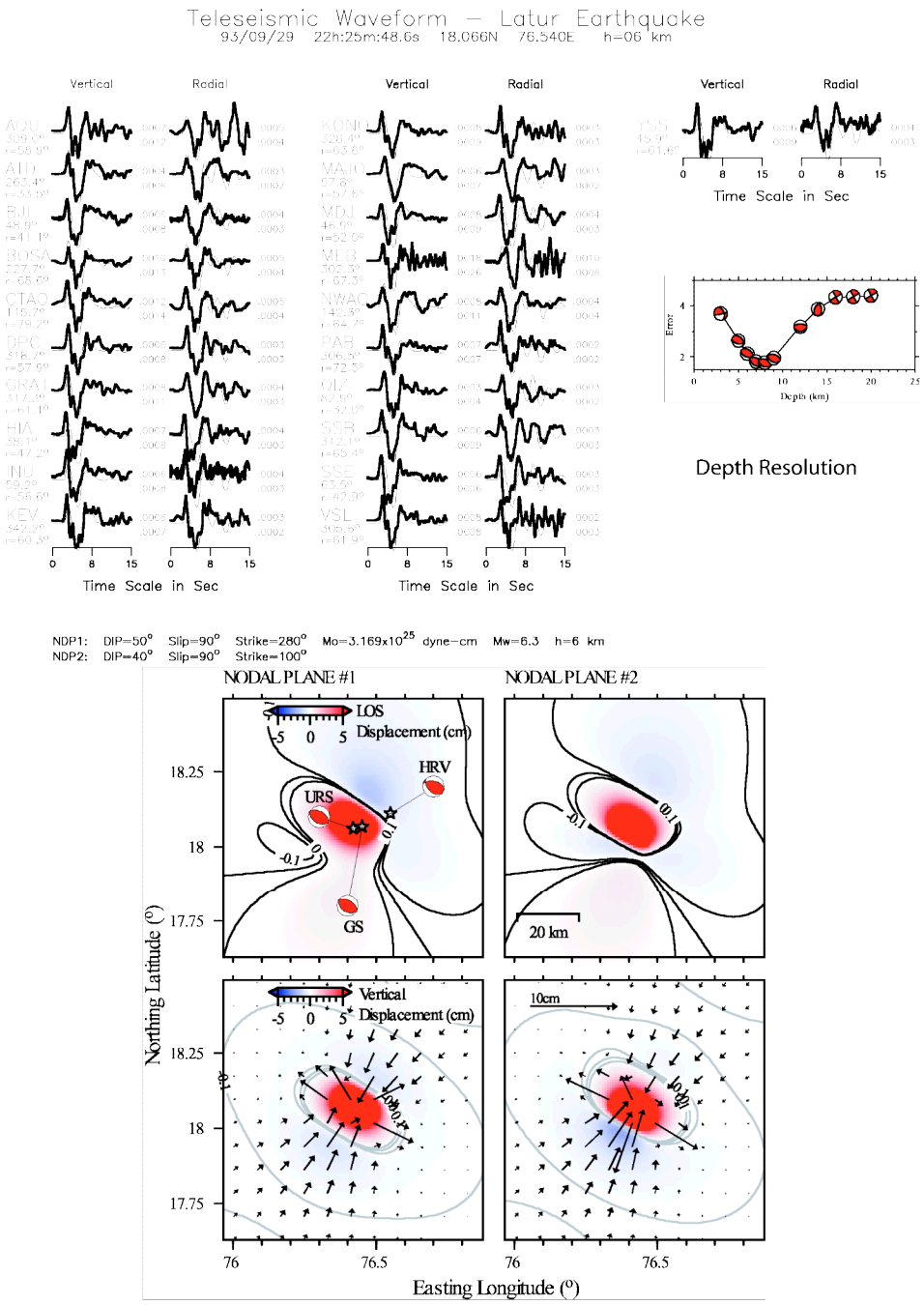

Figure 2. (a) Teleseismic modeling of vertical and radial P waves. Solid traces are the recorded waveforms with instrument response removed. Thin traces correspond to the corresponding synthetic seismograms. (b) LOS (upper) and total (bottom) displacements calculated for the nodal plane 1 (left) and nodal plane (2) right.

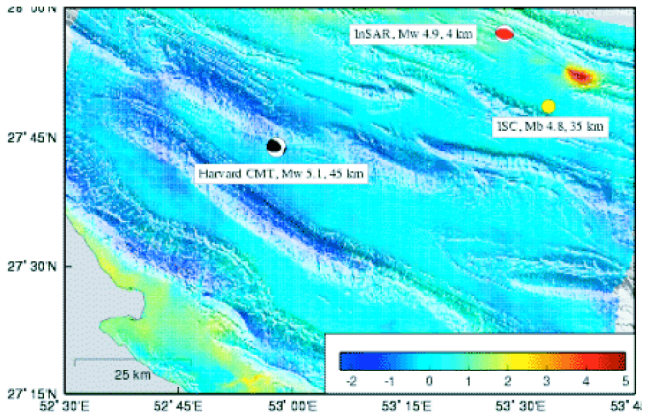

Figure 3. Example showing the seismic locations for the April 30, 1999 southern Iran (Mw 4.8) earthquake relative to the surface deformation observed from the satellite data (elliptical lobe, abot 5 cm surface deformation). Note the location error as well as its error in depth (Harvard nd ISC).

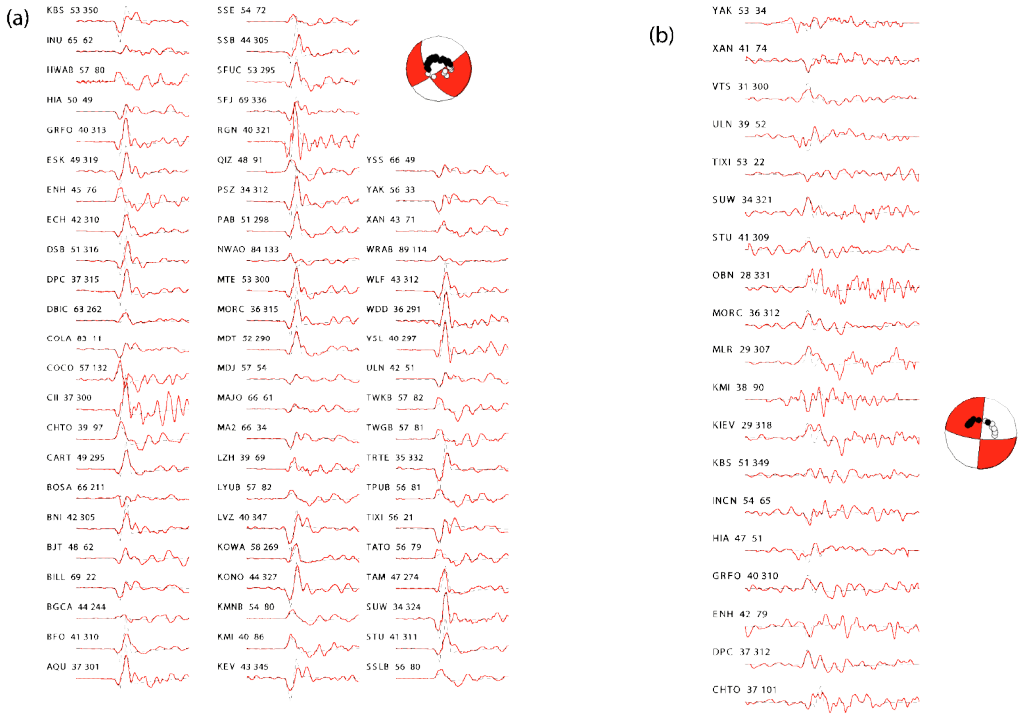

Figure 4. Modeling of teleseismic vertical P waves for (a) March 14, 1998 (Mw=6.6) and (b) June 20, 1997 (Mw=5.6) earthquakes that have occurred in northern and central Iran (red: observed data; dark: syhthetics). Modeling establishes depths of 7 km for the 1998 and 9 km for the 1997nearthquakes. Surface deformation f rom both these earthquakes are observed in satellite data.

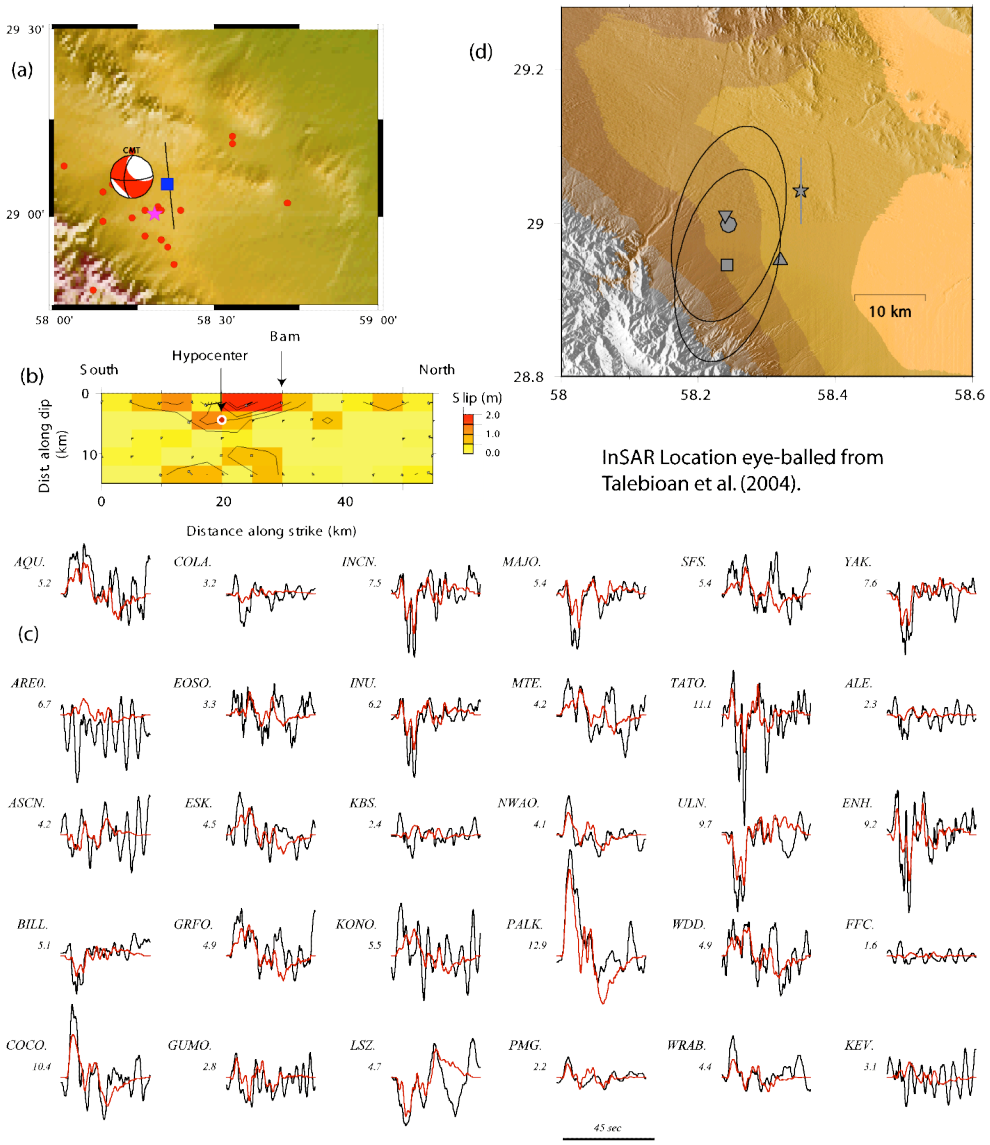

Figure 5. The 2003 Bam earthquake. a - location of the hypocenter (star) and aftershocks (red dots) simplified fault trace and CMT solution. The blue square denotes the city of Bam. b - preliminary slip distribution based on teleseismic body wave inversion. c - observed (black) and synthetic waveforms, d - comparison of different hypocenters, IDC (triangle), Harvard CMT (centroid location, inverted triangle), INSAR (star) and our locations including SSSC's (square) and without SSSC's (circle).